Q. J. Ge[1]
e-mail: Qiaode.Ge@stonybrook.edu

Ping Zhao

Anurag Purwar
e-mail: Anurag.Purwar@stonybrook.edu

Xiangyun Li

Computational Design Kinematics Lab,
Department of Mechanical Engineering,
Stony Brook University,
Stony Brook, NY 11794-2300

A Novel Approach to Algebraic Fitting of a Pencil of Quadrics for Planar 4R Motion Synthesis

The use of the image space of planar displacements for planar motion approximation is a well studied subject. While the constraint manifolds associated with planar four-bar linkages are algebraic, geometric (or normal) distances have been used as default metric for nonlinear least squares fitting of these algebraic manifolds. This paper presents a new formulation for the manifold fitting problem using algebraic distance and shows that the problem can be solved by fitting a pencil of quadrics with linear coefficients to a set of image points of a given set of displacements. This linear formulation leads to a simple and fast algorithm for kinematic synthesis in the image space. [DOI: 10.1115/1.4007447]

1 Introduction

This paper deals with the use of the image space of kinematic mapping for planar motion approximation. The concept of kinematic mapping was first introduced by Blaschke [1] and Grunwald [2]. A comprehensive theory for applying kinematic mapping for motion approximation was developed by Ravani and Roth [3,4]. These works were followed by Bodduluri and McCarthy [5], Bodduluri [6], Larochelle [7,14], Ge and Larochelle [8], Husty et al. [9]. Purwar et al. [10] and Wu et al. [11] have applied kinematic mapping approach to the design of single- and multi-DOF (degrees of freedom) planar linkages using an interactive computer graphics method. The basics of kinematic mapping have been summarized in the seminal book by Bottema and Roth [12] and in a more recent book by McCarthy [13].

The main idea of the kinematic mapping based approach to kinematic synthesis is to transform planar displacements into points in the image space and algebraic constraints into algebraic manifolds in the same space. In this way, a single degree of freedom motion of a planar mechanism is represented by the intersection curve of two algebraic manifolds. The problem of motion approximation is transformed into an algebraic curve fitting problem in the image space, where various methods in approximation theory may be applied. This includes the definition of the approximation error (called structural error) in the image space, formulation of a least squares problem, and applying appropriate numerical methods to find values of the design variables for minimization of the error.

While the constraint manifolds associated with planar four-bar linkages are algebraic, geometric (or normal) distances have been used as default metric for least squares fitting of these algebraic manifolds. This paper studies the problem of using algebraic distance for least squares fitting of quadrics defining the constraint manifolds. In contrary to the existing approach of trying to use the intersection curve of two algebraic manifolds for curve fitting, this paper shows that the problem of kinematic synthesis of planar 4R linkages can be solved by directly fitting a pencil of quadrics to a set of image points defining the image curve of a desired motion. This leads to a very simple and fast algorithm for mechanism synthesis. While geometric distance based least squares approximation in theory should yield more accurate approximation, in practice, due to nonlinear nature of the optimization process, approximation of geometric distance is typically used instead of the exact distance. The quality of approximation under algebraic fitting could be actually better than the first order approximation of geometric distances used in prior work.

The organization of the paper is as follows. Section 2 reviews the concept of kinematic mapping and image space in so far as necessary for the development of this paper. Section 3 presents the constraint manifold associated with a planar dyad composed of revolute joints. Section 4 reviews the existing work on least squares fitting of algebraic manifolds using geometric and algebraic distance measures. Section 5 deals with the problem of algebraic fitting of a pencil of quadric surfaces to a set of image points of a set of given displacements. Examples are presented in Sec. 6.

2 The Image Space of Planar Kinematics

A planar displacement, as shown in Fig. 1, can be given by the following 3×3 homogenous matrix:

$$[T] = \begin{bmatrix} \cos\phi & -\sin\phi & d_1 \\ \sin\phi & \cos\phi & d_2 \\ 0 & 0 & 1 \end{bmatrix} \tag{1}$$

where d_1, d_2 represent the origin of the moving frame M with respect to the fixed frame F, and ϕ denotes the orientation of M

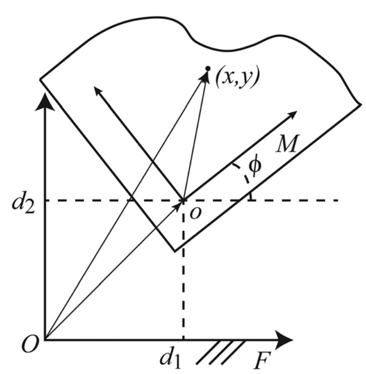

Fig. 1 A planar displacement of a moving frame *M* with respect to the fixed frame *F*

[1]Corresponding author.

Contributed by the Computers and Information Division of ASME for publication in the Journal of Computing and Information Science in Engineering. Manuscript received March 21, 2012; final manuscript received July 28, 2012; published online September 18, 2012. Assoc. Editor: Bahram Ravani.

relative to F. The three parameters (d_1, d_2, ϕ), for a planar displacement can be combined to define a four-dimensional vector $\mathbf{Z} = (Z_1, Z_2, Z_3, Z_4)$ where (see Refs. [3,12,13])

$$
\begin{aligned}
Z_1 &= \frac{1}{2}\left(d_1 \sin\frac{\phi}{2} - d_2 \cos\frac{\phi}{2}\right) \\
Z_2 &= \frac{1}{2}\left(d_1 \cos\frac{\phi}{2} + d_2 \sin\frac{\phi}{2}\right) \\
Z_3 &= \sin\frac{\phi}{2} \\
Z_4 &= \cos\frac{\phi}{2}
\end{aligned}
\tag{2}
$$

In this way, we can convert the homogeneous transform (1) into a new matrix which is quadratic in terms of Z_i ($i = 1, 2, 3, 4$)

$$
[T] = \begin{bmatrix} Z_4^2 - Z_3^2 & -2Z_3Z_4 & 2(Z_1Z_3 + Z_2Z_4) \\ 2Z_3Z_4 & Z_4^2 - Z_3^2 & 2(Z_2Z_3 - Z_1Z_4) \\ 0 & 0 & Z_3^2 + Z_4^2 \end{bmatrix}
\tag{3}
$$

The four-dimensional vector $\mathbf{Z} = (Z_1, Z_2, Z_3, Z_4)$ has been considered as defining a point in a projective three-space called the *Image Space* of planar displacement [3].

3 Algebraic Manifolds in the Image Space

This section provides a review of the constraint manifold associated with a special motion in a plane that has two degrees of freedom: a motion for which a point of the moving body stays on a circle [3,12,13]. Physically, this motion can be realized with a dyad composed of two revolute joints, i.e., an RR dyad.

Let $(x, y, 1)$ denote the homogeneous coordinates of a point on the moving body and (X, Y) its corresponding affine coordinates with respect to the fixed frame. It follows from Eq. (3) that

$$
\begin{aligned}
X &= \frac{(Z_4^2 - Z_3^2)x - 2Z_3Z_4y + 2(Z_1Z_3 + Z_2Z_4)}{Z_3^2 + Z_4^2}, \\
Y &= \frac{2Z_3Z_4x + (Z_4^2 - Z_3^2)y + 2(Z_2Z_3 - Z_1Z_4)}{Z_3^2 + Z_4^2}
\end{aligned}
\tag{4}
$$

Consider a circle with radius r and center at (X_c, Y_c). The substitution of (X, Y) from Eq. (4) into the following equation:

$$
(X - X_c)^2 + (Y - Y_c)^2 - r^2 = 0
\tag{5}
$$

leads to

$$
\begin{aligned}
&Z_1^2 + Z_2^2 + 2\sigma_1Z_1Z_3 + 2\sigma_2Z_2Z_3 + 2\tau_1Z_1Z_4 + 2\tau_2Z_2Z_4 \\
&\quad + 2(\sigma_1\tau_1 + \sigma_2\tau_2)Z_3Z_4 + (\sigma_1^2 + \sigma_2^2 - c)Z_3^2 + (\tau_1^2 + \tau_2^2 - c)Z_4^2 = 0
\end{aligned}
\tag{6}
$$

where

$$
\begin{aligned}
&\sigma_1 = -\frac{x + X_c}{2}, \quad \sigma_2 = -\frac{y + Y_c}{2}, \\
&\tau_1 = -\frac{y - Y_c}{2}, \quad \tau_2 = \frac{x - X_c}{2}, \quad c = \frac{r^2}{4}
\end{aligned}
\tag{7}
$$

In matrix form, Eq. (6) can be expressed as

$$
\mathbf{Z}^{\mathbf{T}}[C]\mathbf{Z} = 0
\tag{8}
$$

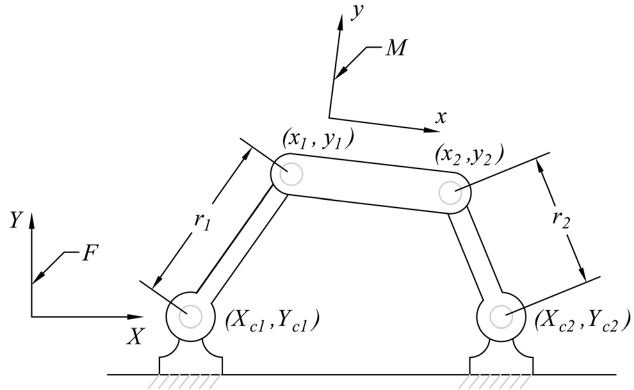

Fig. 2 A planar 4R linkage with a fixed frame *F* and a moving frame *M*. The ground pivots are located at (–2.2, 0.1) and (1.15, 0.38) relative to *F*; the moving pivots are located at (1.24, 0.1) and (4.59, 1.34) relative to *M*; and the length of the input link and output links are $r_1 = 1.2377$ and $r_2 = 4.6712$, respectively.

where

$$
[C] = \begin{bmatrix} 1 & 0 & \sigma_1 & \tau_1 \\ 0 & 1 & \sigma_2 & \tau_2 \\ \sigma_1 & \sigma_2 & \sigma_1^2 + \sigma_2^2 - c & (\sigma_1\tau_1 + \sigma_2\tau_2) \\ \tau_1 & \tau_2 & (\sigma_1\tau_1 + \sigma_2\tau_2) & \tau_1^2 + \tau_2^2 - c \end{bmatrix}
\tag{9}
$$

and $\mathbf{Z}^{\mathbf{T}}$ is a row vector of its coordinates Z_i. This quadric surface has been called the *constraint manifold* of a RR dyad [13]. By letting $Z_4 = 1$, one can rewrite Eq. (6) into

$$
\frac{(Z_1 + \sigma_1Z_3 + \tau_1)^2}{c} + \frac{(Z_2 + \sigma_2Z_3 + \tau_2)^2}{c} - Z_3^2 = 1
\tag{10}
$$

Equation (10) indicates that the projection of the constraint manifold (6) onto the hyperplane $Z_4 = 1$ results in a right circular hyperboloid of one sheet.

For a planar 4R linkage, the coupler motion is constrained by two RR dyads and thus its image curve is the intersection of two constraint manifolds associated with two RR dyads [3]. Figure 2 shows a 4R linkage to be used as an example in Sec. 6 of the paper. Figure 4 shows a pair of hyperboloids of one sheet, which are the constraint manifolds of the linkage. The location, orientation, and size of each of the two hyperboloids are defined by a set of five design variables: three coming from the circle constraints (X_c, Y_c, r) and the other two from the choice of the moving point (x, y). In this way, the problem of dimensional synthesis of a planar 4R linkage for motion approximation can be studied as a curve fitting problem in the image space, i.e., find ten design parameters $(X_{ci}, Y_{ci}, r_i, x_i, y_i)$ ($i = 1, 2$) such that a measurement for motion approximation error is minimized.

4 Least-Square Fitting of Algebraic Manifolds

Ravani and Roth [3] were the first to use normal distance for least squares fitting of a set of image points to the algebraic manifolds of a four-bar motion. Their algorithm has two features: (1) fit the set of image points to two constraint manifolds simultaneously; and (2) use a linear approximation of constraint manifolds to obtain an estimate for the normal distance. The resulting algorithm is highly nonlinear and requires many initial choices to converge to a reasonable solution.

Larochelle [18,19] presented a different approach to the constraint manifold fitting problem that has the following two features: (1) fit the set of image points to a single constraint manifold; and (2) use a direct search method to obtain the normal distance directly. The restriction to a single manifold greatly reduces the difficulty in the fitting problem and only one random initialization is required to converge to a good solution for a single RR dyad. However, the fitting of a single manifold is not sufficient to solve the motion approximation problem that involves the intersection of two manifolds.

The problem of fitting algebraic manifolds (or surfaces) has also received considerable attention in Computer Aided Design (CAD) and pattern recognition. Pratt [15] discussed in details issues related to the least squares fitting of quadric surfaces using algebraic distances. Chen and Liu [16] presented a method for fitting a general quadric surface with ten linear coefficients based on algebraic distance. In particular, they described criteria for classifying various quadric surfaces for surface recognition. Ahn et al. [17] presented a general theory for orthogonal (or normal) distance fitting of implicit curves and surfaces.

Although not explicitly mentioning algebraic distance, Hayes et al. [20,21] explored the use of algebraic distance for least squares fitting of quadric surfaces in the image space of planar kinematics. Hayes and Rusu [21] considered two types of quadrics, one is the general quadric with ten linear coefficients and the other is the constraint manifold associated with a planar dyad. Similar to Chen and Liu [16], they also include a classification of quadric surfaces that are well known in classical geometry. While these ideas present a significant step forward, they did not address the key issue of how the fitting of a single manifold can lead to the complete solution of fitting a set of the image points to the intersection curve of two constraint manifolds.

In summary, there have been two major issues involved in least squares fitting of constraint manifolds: one is the choice of distance measure, geometric or algebraic, and the other is whether to fit a single constraint manifold or two simultaneously. We have found that in the case of constraint manifold of an RR dyad (Eq. (8)), algebraic distance formulation gives almost the same accuracy as geometric distance formulation while incurring far less computational cost. Table 1 lists the results of three fitting methods, the approximate geometric distance fitting of Ravani and Roth [3], the exact geometric distance fitting of Larochelle [18], and the algebraic distance fitting using the Levenberg-Marquardt nonlinear least squares algorithm that we tested. This table uses the input data for the numerical example presented in Ravani and Roth [3].

Furthermore, all the existing work for quadric surface fitting in CAD deals with surface data that lead to a unique best fit surface. In kinematics, however, a given motion is mapped to a curve in the image space. Thus, the problem of quadric surface fitting in the context of kinematic mapping is fundamentally different from CAD. Since only curve data are given, the result is not a unique quadric but a pencil of quadrics that share the same curve of intersection. In this paper, we study algebraic fitting of quadric surfaces from this perspective and develop a new method for kinematic synthesis of planar 4R linkages based on linear least squares fitting of a pencil of quadrics.

5 Algebraic Fitting of a Pencil of Quadrics

A general quadric surface in the Image Space is given by

$$q_1 Z_1^2 + q_2 Z_2^2 + q_3 Z_3^2 + q_4 Z_1 Z_2 + q_5 Z_1 Z_3 + q_6 Z_2 Z_3 + q_7 Z_1 Z_4 + q_8 Z_2 Z_4 + q_9 Z_3 Z_4 + q_{10} Z_4^2 = 0 \quad (11)$$

Table 1 Comparison of geometric versus algebraic distance fitting: $\mathcal{R}$—Ravani, $\mathcal{L}$—Larochelle, $\mathcal{A}$—Algebraic

	(X_c, Y_c, r, x, y)	Structural error
$\mathcal{R}$	(14.00, −0.12, 8.31, 9.00, −1.00)	1.03×10^{-2}
$\mathcal{L}$	(14.98, −2.08, 6.45, 11.22, −4.62)	3.62×10^{-3}
$\mathcal{A}$	(14.92, −2.07, 6.41, 11.03, −4.70)	9.58×10^{-4}

It follows from Eq. (6) that for Eq. (11) to represent the constraint manifold of a RR dyad, we must have

$$q_1 = q_2, \quad q_4 = 0 \quad (12)$$

Substituting the above into Eq. (11) and replacing the remaining coefficients with $p_i (i = 1, 2, \ldots, 8)$, we obtain

$$p_1(Z_1^2 + Z_2^2) + p_2 Z_3^2 + p_3 Z_1 Z_3 + p_4 Z_2 Z_3 + p_5 Z_1 Z_4 + p_6 Z_2 Z_4 + p_7 Z_3 Z_4 + p_8 Z_4^2 = 0 \quad (13)$$

Let $X = Z_1/Z_4, Y = Z_2/Z_4, Z = Z_3/Z_4$. Now, consider the problem of fitting a pencil of quadrics to a set of N points, where $N > 8$, arranged such that they define an image curve rather than a surface. This problem can be formulated as an overconstrained linear problem $[A]\mathbf{p} = 0$ where the coefficient matrix becomes the matrix $[A]$, which is given by

$$[A] = \begin{bmatrix} X_1^2 + Y_1^2 & Z_1^2 & X_1 Z_1 & Y_1 Z_1 & X_1 & Y_1 & Z_1 & 1 \\ \vdots & & & & & & & \vdots \\ \vdots & & & & \ddots & & & \vdots \\ \vdots & & & & & & & \vdots \\ X_N^2 + Y_N^2 & Z_N^2 & X_N Z_N & Y_N Z_N & X_N & Y_N & Z_N & 1 \end{bmatrix} \quad (14)$$

5.1 Singular Value Decomposition (SVD). In linear algebra, the SVD of an $N \times 8$ matrix $[A]$ is a factorization of the form [22]

$$[A] = [U][S][V]^T \quad (15)$$

where $[U]$ is an $N \times N$ orthonormal matrix, whose N columns, called the *left singular vectors* of $[A]$, are the eigenvectors of $[A][A]^T$; $[S]$ is an $N \times 8$ diagonal matrix with eight non-negative real numbers (singular values) on the diagonal, whose values are square roots of the eigenvalues of $[A][A]^T$ (or, $[A]^T[A]$); and $[V]^T$ is an 8×8 orthonormal matrix, whose eight columns, called the *right singular vectors*, are the eigenvectors of $[A]^T[A]$.

The overconstrained system of linear equations, $[A]\mathbf{p} = 0$, can be solved as a total least squares minimization problem with the constraint $\mathbf{p}^T\mathbf{p} = 1$. The solution turns out to be the right singular vector of $[A]$ corresponding to the smallest singular value. For a two-dimensional set of points (or surface data), if there is a perfect fit, there will be only one singular value that is equal to zero. This leads to a unique singular vector that defines the coefficients of a quadric that best fits the data; for a one-dimensional set of points (or curve data), if there is a perfect fit, there will be two singular values that are zero. In this case, they lead to a singular plane, which may be defined by a pair of orthonormal singular vectors of eight dimensions, $\mathbf{v}_1$ and $\mathbf{v}_2$, that correspond to two smallest

Table 2 Ten positions sampled from a four-bar motion

Translation	Rotation (deg)
(−0.8253,−1.0329)	91.91
(−1.6554, −0.2721)	66.99
(−2.6392,0.2920)	49.90
(−3.5027,0.3088)	43.94
(−4.0549, −0.2141)	45.58
(−4.1022, −1.0521)	52.67
(−3.5805, −1.8708)	64.52
(−2.6250, −2.3408)	78.84
(−1.5557, −2.2742)	93.02
(−0.8016, −1.7382)	101.25

Table 3 The singular values of $[A]$

4.48×10^{-8}	5.91×10^{-8}	0.0073	0.1525	0.2868	1.2043	1.6355	10.4664

singular values. Thus, any unit vector in the singular plane can be given by

$$\mathbf{p} = \cos\theta\mathbf{v}_1 + \sin\theta\mathbf{v}_2 \tag{16}$$

where the angle θ indicates the orientation of $\mathbf{p}$ relative to the basis vectors $\mathbf{v}_1$ and $\mathbf{v}_2$. In view of Eq. (13), the singular vector $\mathbf{p}$ given by Eq. (16) defines a pencil of quadrics as θ varies.

5.2 Identifying Constraint Manifolds From a Pencil of Quadrics. We note that the singular vectors, $\mathbf{v}_1$ and $\mathbf{v}_2$, obtained directly from a SVD algorithm may not take the form of the constraint manifold associated with a RR dyad as given by Eq. (6). As can be seen in Sec. 6 (Fig. 4), in addition to a hyperboloid of one sheet, Eq. (13) may yield an ellipsoid or an hyperboloid of two sheets as well. We now consider the problem of identifying those special quadrics within the pencil of quadrics that correspond to the constraint manifold of a RR dyad. By comparing Eqs. (6) with (13), we conclude that a singular vector (16) represents the coefficients of a constraint manifold when their components satisfy the following two quadratic relations:

$$\begin{aligned} &p_1p_7 - (p_3p_5 + p_4p_6)/2 = 0,\\ &p_1(p_2 - p_8) - (p_3^2 + p_4^2 - p_5^2 - p_6^2)/4 = 0 \end{aligned} \tag{17}$$

When the given data are perfect, i.e., when they are generated from a RR dyad, the two relations in Eq. (17) would be compatible. If the data are not perfect, we may have to find the angle θ that approximately satisfies Eq. (17). This may be formulated as a least squares problem

$$\begin{aligned} E(\theta) = {}&[p_1p_7 - (p_3p_5 + p_4p_6)/2]^2\\ &+ [p_1(p_2 - p_8) - (p_3^2 + p_4^2 - p_5^2 - p_6^2)/4]^2 \end{aligned} \tag{18}$$

The optimal value for θ can be obtained by minimizing $E(\theta)$.

6 Three Examples

6.1 Exact Four-Bar Motion Synthesis. In this section, we use an example of a four-bar coupler motion that comes from Fig. 2 to illustrate our approach. Listed in the caption are the parameters that constrain this four-bar motion. These include the centers and radii of two circles, $(X_{c1}, Y_{c1}), (X_{c2}, Y_{c2}), r_1$ and r_2 as well as the locations of moving pivots (x_1, y_1) and (x_2, y_2) with respect to the moving frame.

We sample ten positions from this motion and list them in Table 2. The size for matrix $[A]$ as in Eq. (14) is 10×8. The next step is to find the two smallest singular values and their corresponding singular vectors of $[A]$ by SVD. The singular values are listed as in Table 3. Two near-zero singular values close to the machine precision are $\sigma_1 = 4.48\times10^{-8}, \sigma_2 = 5.91\times10^{-8}$. Their associated singular vectors are listed in Table 4, where the last column e indicates the square-root of the constraint fitting error E

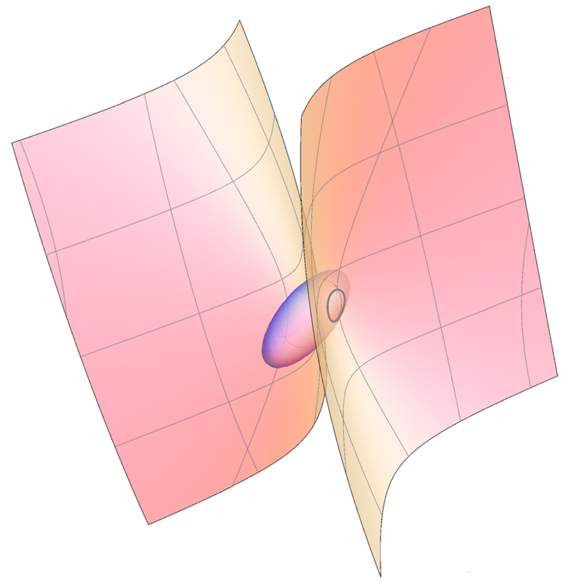

Fig. 3 Two "eigen-quadrics" defined by two singular vectors in Table 4: $\mathbf{v}_1$ defines an ellipsoid while $\mathbf{v}_2$ defines a hyperboloid of two sheets. The highlighted image curve shows the intersection of two quadrics.

as defined by (18). As shown in Fig. 3, these singular vectors define an ellipsoid and a hyperboloid of two sheets and, therefore, are not the constraint manifolds of RR dyads.

Minimizing $E(\theta)$ in Eq. (18) leads to two sets of solution as listed below

$$\begin{aligned} &\theta_1 = -43.13\,\text{deg}, \quad e_1 = 2.25\times10^{-11},\\ &\theta_2 = 44.72\,\text{deg}, \quad e_2 = 6.98\times10^{-13} \end{aligned} \tag{19}$$

They give rise to the following two coefficient matrices:

$$[C_1] = \begin{bmatrix} 1 & 0 & 0.4800 & 0.0000\\ 0 & 1 & -0.1000 & 1.7200\\ 0.4800 & -0.1000 & -0.1426 & -0.1720\\ 0.0000 & 1.7200 & -0.1720 & 2.5754 \end{bmatrix} \tag{20}$$

$$[C_2] = \begin{bmatrix} 1 & 0 & -2.8700 & -0.4800\\ 0 & 1 & -0.8600 & 1.7200\\ -2.8700 & -0.8600 & 3.5215 & -0.1016\\ -0.4800 & 1.7200 & -0.1016 & -2.2662 \end{bmatrix} \tag{21}$$

The constraint manifolds defined by these two matrices are shown in Fig. 4. They represent exactly the two hyperboloids of one sheet that constrain the motion of the given four-bar mechanism.

We also note that quadrics in Figs. 3 and 4 share the same intersection curve, yet only a pair of them are valid constraint manifolds. Since vector $\mathbf{p}$ in Eq. (16) represents an arbitrary vector in the singular plane, we can visualize the evolution of the "eigen-quadrics" to the constraint manifolds by varying θ. Figure 5 shows

Table 4 A pair of orthonormal singular vectors corresponding to singular values $\sigma_1 = 4.48\times10^{-8}$ and $\sigma_2 = 5.91\times10^{-8}$. Error e in the last column indicates the constraint fitting error.

	p_1	p_2	p_3	p_4	p_5	p_6	p_7	p_8	e
$\mathbf{v}_1$	0.2387	0.2716	−0.3298	−0.1745	−0.8009	0.8211	−0.0704	0.2108	0.1555
$\mathbf{v}_2$	−0.0677	0.3360	−0.6618	−0.1218	−0.0855	−0.2329	0.0358	−0.6057	0.1677

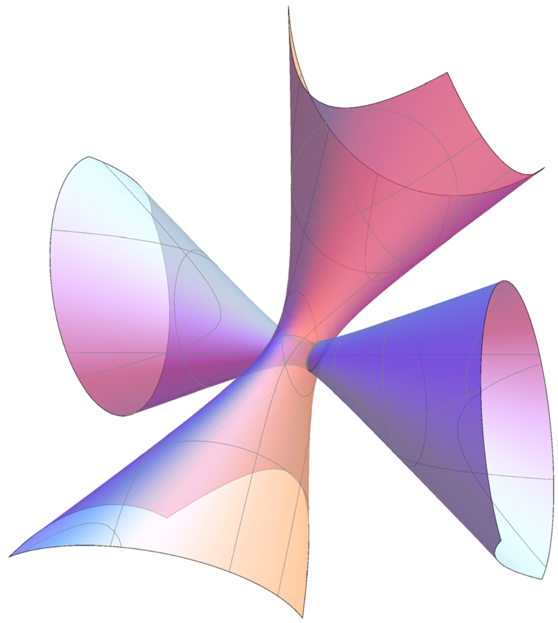

Fig. 4 Constraint manifolds of the two dyads identified from a pencil of quadrics. In the hyperplane $Z_4 = 1$, the two constraint manifolds are given by $(X+22)^2+(Y - 01)^2=1.53$ and $(X+115)^2+(Y\text{-}038)^2=21.82$.

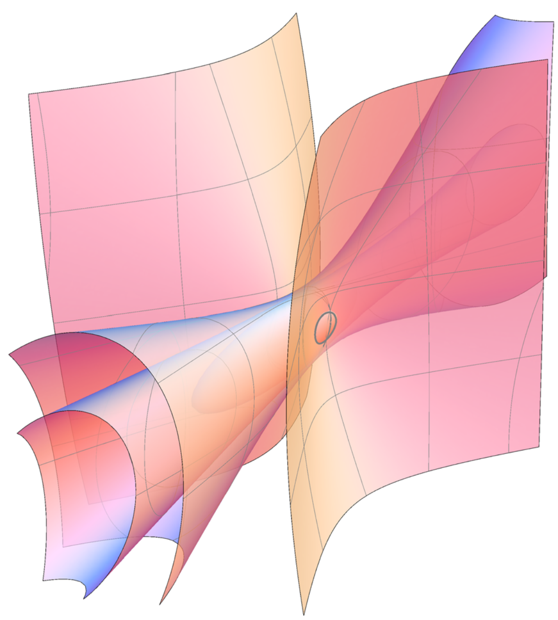

Fig. 5 *In-between* quadrics obtained from vector p for three values of $\theta = 80.21$ deg, 70.73 deg, 60.00 deg. Also, shown is an "eigen-quadric" (hyperboloid of two sheets) defined by v_2 ($\theta = 90$ deg).

how the ellipsoid of Fig. 3 evolves to a hyperboloid of one sheet that represents a valid circular constraint. Similarly, Fig. 6 shows how the hyperboloid of two sheets in Fig. 3 evolves to a hyperboloid of one sheet.

6.2 Approximate Four-Bar Motion Synthesis. In this section, to illustrate how well our approach handles approximated motion, we add some random noise to the input positions given in Table 2. The new data are listed in Table 5.

Following the same procedure as before, we obtain the singular values as listed in Table 6. Two near-zero singular values

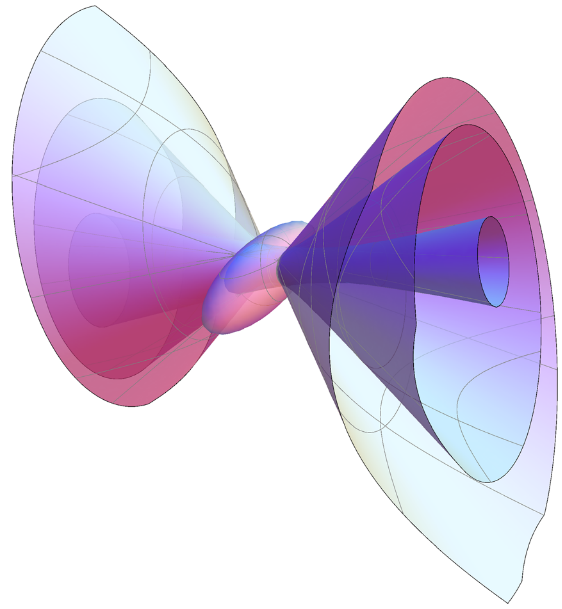

Fig. 6 *In-between* quadrics obtained from vector *p* for three values of $\theta = -48.60$ deg, -42.84 deg, -36.87 deg. Also, shown is an "eigen-quadric" (ellipsoid) defined by v_1 ($\theta = 0$).

Table 5 Ten given positions for approximate motion synthesis

Translation	Rotation (deg)
(−0.9822, −1.0389)	78.54
(−1.6808, −0.2377)	56.77
(−2.5539,0.3288)	42.43
(−3.3366,0.3632)	37.77
(−3.8565, −0.1174)	39.89
(−3.9009, −0.9078)	47.13
(−3.4396, −1.6997)	58.25
(−2.5710, −2.1842)	71.48
(−1.6143, −2.1793)	83.77
(−0.9229, −1.7280)	89.21

Table 6 The singular values of [*A*] for the approximated example

1.76×10^{-3}	3.03×10^{-3}	0.0696	0.1336	0.1533	1.1662	1.5327	9.7251

are: $\sigma_1 = 1.76 \times 10^{-3}, \sigma_2 = 3.03 \times 10^{-3}$ and their associated singular vectors as well as the constraint fitting error e are listed in Table 7.

Minimizing the error function in Eq. (18) leads to

$$\begin{aligned} \theta_1 &= -21.28 \text{ deg}, \quad e_1 = 5.78 \times 10^{-3} \\ \theta_2 &= 54.08 \text{ deg}, \quad e_2 = 5.65 \times 10^{-3} \end{aligned} \tag{22}$$

The resulting singular vectors define the constraint manifolds with the following coefficient matrices:

$$[C_1] = \begin{bmatrix} 1 & 0 & 0.3597 & 0.03519 \\ 0 & 1 & -0.1420 & 1.6281 \\ 0.3597 & -0.1420 & -0.1341 & -0.2709 \\ 0.03519 & 1.6281 & -0.2709 & 2.3668 \end{bmatrix} \tag{23}$$

Table 7 A pair of orthonormal singular vectors that correspond to singular values $\sigma_1 = 1.76\times10^{-3}$ and $\sigma_2 = 3.03\times10^{-3}$. Error e in the last column indicates their constraint fitting error.

	p_1	p_2	p_3	p_4	p_5	p_6	p_7	p_8	e
$\mathbf{v}_1$	0.2385	0.1986	−0.08753	−0.1188	0.007753	0.7819	−0.2153	0.4734	0.08199
$\mathbf{v}_2$	−0.03487	0.5966	−0.6903	−0.1211	−0.02564	−0.1002	−0.2019	−0.3166	0.1522

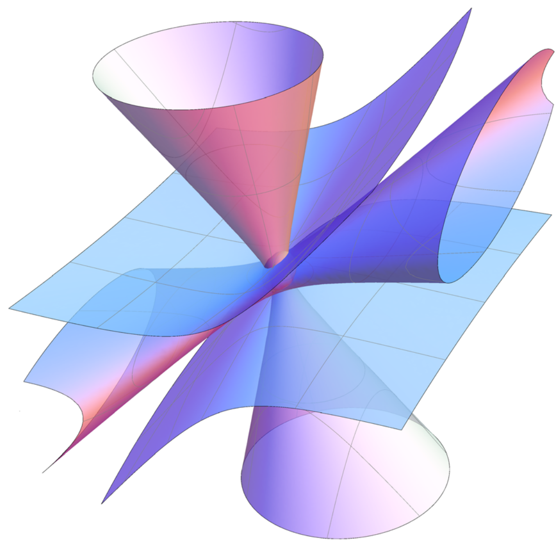

Fig. 7 "Eigen-quadrics" (ellipsoid and hyperboloid of two sheets) and the constraint manifolds (hyperboloid of one sheet) of a planar 4R mechanism for approximate motion synthesis

Table 8 The resulting parameters of a planar 4R mechanism for approximate motion synthesis

Design variables	Value
(X_{c1}, Y_{c1})	$(-1.9878, 0.1772)$
r_1	1.0667
(x_1, y_1)	(1.2684,0.1068)
(X_{c2}, Y_{c2})	(1.0431,0.6785)
r_2	3.2664
(x_2, y_2)	(4.4231,0.8237)

Table 9 Comparison of resulting parameters of a planar 4R mechanism with Ravani and Roth's example

Design variables	Our method	Ravani
(X_{c1}, Y_{c1})	$(6.43, -0.21)$	$(6.46, -0.06)$
r_1	5.02	5.07
(x_1, y_1)	$(2.73, -8.60)$	$(3, -9)$
(X_{c2}, Y_{c2})	$(15.00, -0.80)$	$(14.00, -0.12)$
r_2	5.97	8.31
(x_2, y_2)	$(11.40, -4.33)$	$(9.00, -1.00)$

$$[C_2] = \begin{bmatrix} 1 & 0 & -2.7331 & 0.07263 \\ 0 & 1 & -0.7511 & 1.6900 \\ -2.7331 & -0.7511 & 5.3699 & -1.2975 \\ 0.07263 & 1.6900 & -1.2975 & 0.1907 \end{bmatrix} \quad (24)$$

Figure 7 show two "eigen-quadrics" as well as two constraint manifolds. The mechanism parameters can be obtained from Eq. (9) and are listed in Table 8. The structural error of approximation is calculated to be 8.41×10^{-2}.

6.3 Comparison With Ravani and Roth's [3] Example. For Ravani and Roth's [3] ten design positions, our linear optimization method produces structural error of 9.51×10^{-3}, which is only slightly lower than their error of 1.03×10^{-2}, however, the advantage over their method is in a simpler and efficient formulation. Table 9 lists the results of the comparison between our method and Ravani and Roth's method.

7 Conclusions

In this paper, we presented a novel method for synthesizing planar motion using kinematic mapping. Instead of finding two constraint manifolds associated with a four-bar linkage with nonlinear (quadratic) coefficients, which makes the problem difficult to solve, we used a more general form of quadric such that its coefficients are linear. Furthermore, we seek to fit a given set of image points to a pencil of quadrics. This leads to a linear least squares problem that can be readily solved using SVD algorithm. After obtaining the pencil of quadrics that contains the constraint manifolds, we then impose the quadratic constraints associated with the constraint manifold to find the two special quadrics that satisfy the requirements for a RR dyad. The resulting algorithm for planar four-bar linkage synthesis is efficient and the underlying mathematical machinery is simpler.

Acknowledgment

The work has been financially supported by National Science Foundation under Collaborative Research grant to Stony Brook University (Q. J. Ge, Grant No. CMMI-0856594). All findings and results presented in this paper are those of the authors and do not represent those of the funding agencies.

References

[1] Blaschke, W., 1911, "Euklidische kinematik und nichteuklidische geometrie," Zeitschr. Math. Phys., **60**, pp. 61–91.
[2] Grunwald, J., 1911, "Ein abbildungsprinzip, welches die ebene geometrie und kinematik mit der raumlichen geometrie verknupft," Sitzber. Ak. Wiss. Wien, **120**, pp. 677–741.
[3] Ravani, B., and Roth, B., 1983, "Motion Synthesis Using Kinematic Mappings," ASME J. Mech., Transm., Autom. Des., **105**(3), pp. 460–467.
[4] Ravani, B., and Roth, B., 1984, "Mappings of Spatial Kinematics," ASME J.Mech., Transm., Autom, Des., **106**(3), pp. 341–347.
[5] Bodduluri, R. M. C., and McCarthy, J. M., 1992, "Finite Position Synthesis Using the Image Curve of a Spherical Four-Bar Motion," ASME J. Mech. Des., **114**(1), pp. 55–60.
[6] Bodduluri, R., 1990, "Design and Planned Movement of Multi-Degree of Freedom Spatial Mechanisms," Ph.D. thesis, University of California, Irvine.
[7] Larochelle, P., 1994, "Design of Cooperating Robots and Spatial Mechanisms," Ph.D. thesis, University of California, Irvine.
[8] Ge, Q. J., and Larochelle, P., 1999, "Algebraic Motion Approximation With NURBS Motions and Its Application to Spherical Mechanism Synthesis," J. Mech. Des., **121**(4), pp. 529–532.
[9] Husty, M. L., Pfurner, M., Schrocker, H.-P., and Brunnthaler, K., 2007, "Algebraic Methods in Mechanism Analysis and Synthesis," Robotica, **25**, pp. 661–675.
[10] Purwar, A., Anantwar, S., and Zhao, P., 2012, "An Interactive Approach to Designing Planar Parallel Manipulators Using Image Space Representation," ASME 2012 International Design Engineering Technical Conferences and Computers and Information in Engineering Conference, Chicago, Paper No. DETC2012-70880.

[11] Wu, J., Purwar, A., and Ge, Q. J., 2010, "Interactive Dimensional Synthesis and Motion Design of Planar 6R Single-Loop Closed Chains via Constraint Manifold Modification," ASME J. Mech. Rob., **2**, p. 31012.
[12] Bottema, O., and Roth, B., 1979, *Theoretical Kinematics*, North-Holland, Amsterdam.
[13] McCarthy, J. M., 1990, *Introducation to Theoretical Kinematics*, MIT, Cambridge, MA.
[14] Larochelle, P., 1996, "Synthesis of Planar RR Dyads by Constraint Manifold Projection," Proceedings of the ASME Design Engineering Technical Conferences, Paper No. 96-DETC/MECH-1187, ASME Press, Irvine, CA.
[15] Pratt, V., 1987, "Direct Least-Squares Fitting of Algebraic Surfaces," ACM SIGGRAPH Comput. Graph., **21**(4), pp. 145–152.
[16] Chen, Y. H., and Liu, C. Y., 1999, "Quadric Surface Extraction Using Genetic Algorithms," Comput. Aided Des., **31**(2), pp. 101–110.
[17] Ahn, S. J., Rauh, W., Cho, H. S., and Warnecke, H.-J., 2002, "Orthogonal Distance Fitting of Implicit Curves and Surfaces," IEEE Trans. Pattern Anal. Mach. Intell., **24**(5), pp. 620–638.
[18] Larochelle, P., 2000, "Approximate Motion Synthesis via Parametric Constraint Manifold Fitting," *Advances in Robot Kinematics*, KAP, The Netherlands, pp. 103–110.
[19] Larochelle, P., 2003, "Approximate Motion Synthesis of Open and Closed Chains via Parametric Constraint Manifold Fitting: Preliminary Results," 2003 ASME Design Automation Conference, Sept. 26, Chicago, Illinois, Paper No. DETC2003/DAC-48814, pp. 1049–1057.
[20] Hayes, M. J. D., Luu, T., and Chang, X.-W., 2004, "Kinematic Mapping Application to Approximate Type and Dimension Synthesis of Planar Mechanisms," *Advances in Robotic Kinematics*, J. Lenarcic, and C. Galletti, eds., Kluwer Academic Publishers, Dordrecht, The Netherlands, pp. 41–48.
[21] Hayes, M. J. D., and Rusu, S. R., 2011, "Quadric Surface Fitting Applications to Approximate Dimensional Synthesis," 13th World Congress in Mechanism and Machine Science, June 19–23.
[22] Golub, G., and Van Loan, C., 1996, *Matrix Computations*, Johns Hopkins University Press, Baltimore, MD.